Supporting Information for

Swelling Effect on Yielding, Elasticity and Fracture of Double-Network Hydrogels with Inhomogeneous First Network

Yong Zheng[1], Tasuku Nakajima[1,2], Wei Cui[2,3], Chung-Yuen Hui[4,5] and Jian Ping Gong[1,2,4]*

[1]Institute for Chemical Reaction Design and Discovery (WPI-ICReDD), Hokkaido University, Sapporo 001-0021, Japan

[2]Faculty of Advanced Life Science, Hokkaido University, Sapporo 001-0021, Japan

[3]College of Polymer Science and Engineering, State Key Laboratory of Polymer Materials Engineering, Sichuan University, Chengdu, 610065 China

[4]Global Station for Soft Matter, GI-CoRE, Hokkaido University, Sapporo 001-0021, Japan

[5]Field of Theoretical and Applied Mechanics, Sibley School of Mechanical and Aerospace Engineering, Cornell University, Ithaca, NY 14853, USA

*Corresponding author: gong@sci.hokudai.ac.jp

Table S1. Compositions and λ_s of DN-x-λ_s gels. Monomer concentration (1 M) and initiator concentration (1 mol%) of the first network were kept the same, and the first network crosslinker density x (mol%) was varied. For the second network, monomer concentration (C_{2nd}) was varied and the crosslinker density (0.01 mol%) and initiator density (0.01 mol%) were kept constant. The mol% is relative to the monomer. For the abbreviations "stent-y" and "PEG-z" of the methods used, y represents molecular stent concentration and z represents PEG weight fraction, respectively.

DN-x-λ_s	x (mol%)	C_{2nd} (M)	Stent-y / PEG-z	$\lambda_{s,1}$	$\lambda_{s,3}$	λ_s
DN-3-2.70	3.0	2.0	water	2.50	1.08	2.70
DN-3-2.36			PEG-10wt%		0.94	2.36
DN-3-2.04			PEG-20wt%		0.82	2.04
DN-3-3.32			stent-0.6 M		1.33	3.32
DN-3-3.75			stent-1.2 M		1.50	3.75
DN-3-4.98			stent-2.5 M		1.99	4.98
DN-4.5-2.12	4.5	3.0	water	2.03	1.04	2.12
DN-4.5-2.02			PEG-10wt%		0.99	2.02
DN-4.5-1.66			PEG-20wt%		0.82	1.66
DN-4.5-2.20			stent-0.6 M		1.08	2.20
DN-4.5-2.63			stent-1.2M		1.30	2.63
DN-4.5-3.31			stent-2.5 M		1.63	3.31
DN-4-2.23	4	2.0	water	2.12	1.05	2.23
DN-6-1.82	6	2.0	water	1.78	1.02	1.82

Table S2. Compositions and λ_s of TN-x-λ_s gels.

TN-x-λ_s	x (mol%)	C_{2nd}(M) /C_{3rd} (M)*	Stent-y / PEG-z	$\lambda_{s, 1}$	$\lambda_{s, 2}$	$\lambda_{s, 3}$	λ_s
TN-4.5-2.64			water			1.25	2.64
TN-4.5-2.39			PEG-10wt%			1.13	2.39
TN-4.5-2.12	4.5	3.0/3.0	PEG-20wt%	2.03	1.04	1.0	2.12
TN-4.5-3.11			stent-1.2 M			1.47	3.11
TN-4.5-3.67			stent-2.5 M			1.73	3.67

*The crosslinker density (0.01 mol%) and initiator density (0.01 mol%) for the second and third networks were kept constant.

Table S3. Young's modulus E_0 and the density of the elastically effective strands $v_{e, 0}$ of the as-prepared PAMPS SN-x and TPEG SN. The data for TPEG was from ref.[21].

| SN-x	E_0 (MPa)	$v_{e, 0}$ (m^{-3})
SN-3	0.0209	3.38×10^{24}
SN-4	0.024	3.88×10^{24}
SN-4.5	0.0292	4.73×10^{24}
SN-6	0.0405	6.56×10^{24}
TPEG SN in ref. [21]	0.0439	7.11×10^{24}

Table S4. Theoretical stretching limit of first network strands $\lambda_{max,0}$ and elastic energy per Kuhn segment of strands $\dfrac{F_{el}^0}{N_x k_B T} = \dfrac{2E\lambda_s^{\,3}}{3k_B T C_0}$ for various gels.

|	λ_s	$\lambda_{max,o}$	$\lambda_s/\lambda_{max,o}$	$\dfrac{2E\lambda_s^{\,3}}{3k_B T C_0}$
DN-3-λ_s	2.04	9.44	0.216	0.237
	2.36	9.44	0.250	0.479
	2.70	9.44	0.286	1.499
	3.32	9.44	0.351	3.815
	3.75	9.44	0.397	4.974
	4.98	9.44	0.528	7.574
DN-4.5-λ_s	1.66	7.98	0.209	0.346
	2.02	7.98	0.254	1.309
	2.12	7.98	0.265	2.097
	2.20	7.98	0.275	2.385
	2.63	7.98	0.329	5.399
	3.31	7.98	0.415	7.235
TN-4.5-λ_s	2.12	7.98	0.265	1.678
	2.39	7.98	0.300	4.180
	2.64	7.98	0.331	7.141
	3.11	7.98	0.390	8.599
	3.67	7.98	0.461	10.113
TPEG DN from ref [21]	1.0	7.6	0.131	0.028
	2.1	7.6	0.271	0.174
	2.3	7.6	0.303	0.232
	3.0	7.6	0.382	0.478
	3.3	7.6	0.440	0.744
	3.9	7.6	0.511	1.132

Table S5. A list of fracture energy Γ, yielding zone area S, yielding zone deformation ratio λ_{yz}, yielding zone size h_y, and yielding true stress $\sigma_{T,y}$ for various DN-3-λ_s gels, DN-4.5-λ_s and TN-4.5-λ_s gels.

| Sample code	Γ (J/m²)	S (mm²)	λ_{yz}	h_y (mm)	$\sigma_{T,y}$ (MPa)
DN-3-2.70	3342 ± 655	10.68 ± 2.33	11.0	0.30 ± 0.03	1.70 ± 0.09
DN-3-2.36	3569 ± 74	7.91 ± 1.34	12.6	0.22 ± 0.02	2.46 ± 0.08
DN-3-2.04	7572 ± 3033	16.29 ± 4.09	15.0	0.27 ± 0.03	4.18 ± 0.34
DN-3-3.32	1802 ± 468	6.80 ± 0.96	9.0	0.29 ± 0.02	0.92 ± 0.05
DN-3-3.75	1428 ± 398	17.62 ± 5.33	7.0	0.60 ± 0.09	0.46 ± 0.03
DN-3-4.98	320 ± 3	N.M.	N.M.	N.M.	0.13 ± 0.01
DN-4.5-2.12	2326 ± 326	1.44 ± 0.22	8.5	0.14 ± 0.01	3.08 ± 0.15
DN-4.5-2.02	2586 ± 384	1.87 ± 0.19	9.0	0.15 ± 0.01	3.67 ± 0.08
DN-4.5-1.66	3015 ± 1476	1.88 ± 0.60	11.0	0.12 ± 0.02	6.05 ± 0.43
DN-4.5-2.20	2137 ± 218	1.79 ± 0.58	8.2	0.16 ± 0.03	2.53 ± 0.06
DN-4.5-2.63	1423 ± 212	1.63 ± 0.24	7.5	0.17 ± 0.01	1.69 ± 0.04
DN-4.5-3.31	955 ± 45	0.33 ± 0.02	5.0	0.11 ± 0.00	0.83 ± 0.04
TN-4.5-2.64	1794 ± 368	0.89 ± 0.27	6.0	0.16 ± 0.02	2.40 ± 0.08
TN-4.5-2.39	2463 ± 462	1.17 ± 0.37	6.5	0.17 ± 0.03	2.48 ± 0.03
TN-4.5-2.12	1827 ± 487	1.04 ± 0.07	7.0	0.15 ± 0.01	3.26 ± 0.22
TN-4.5-3.11	894 ± 130	0.84 ± 0.04	4.5	0.20 ± 0.01	1.11 ± 0.09
TN-4.5-3.67	606 ± 132	0.88 ± 0.57	4.0	0.23 ± 0.08	0.55 ± 0.02

N.M. means "not measured".
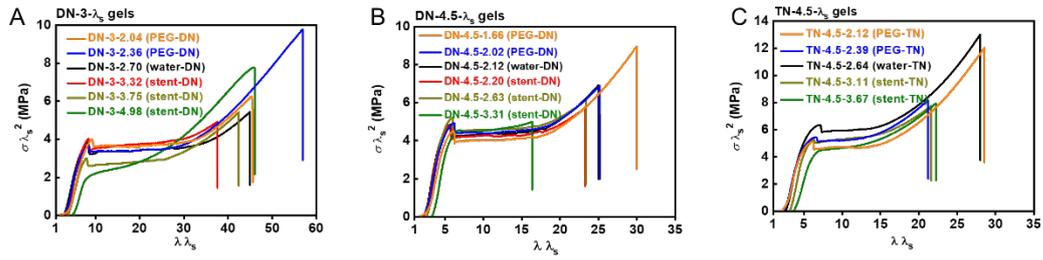
Figure S1. Rescaled tensile behaviors in various series of DN and TN gels. (A-C) Rescaled tensile stress $\sigma\lambda_s{}^2$-stretch ratio $\lambda\lambda_s$ curves for (A) DN-3-λ_s gels, (B) DN-4.5-λ_s gels and (C) TN-4.5-λ_s gels.
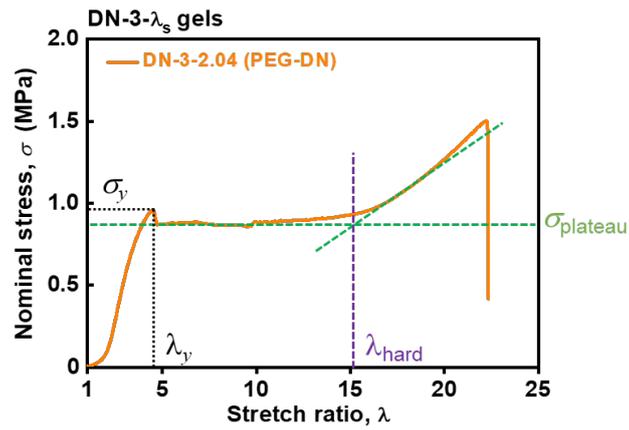
Figure S2. Determination of the parameters λ_y, σ_y, λ_{hard}, $\sigma_{plateau}$ from stress curve (DN-3-2.04 as an example). The yielding stretch ratio and yielding stress at the onset of necking, λ_y and σ_y, were determined as the nominal stretch ratio and stress at the zero-slope point of the nominal stress σ- stretch ratio λ curves, respectively. The plateau stress after yielding, $\sigma_{plateau}$, was determined as the average stress in the plateau stress region; the stretch ratio at the onset of strain-hardening, λ_{hard}, was determined as the crossover point where the linear stress extrapolation curves in the strain-hardening region meet the plateau stress curve.
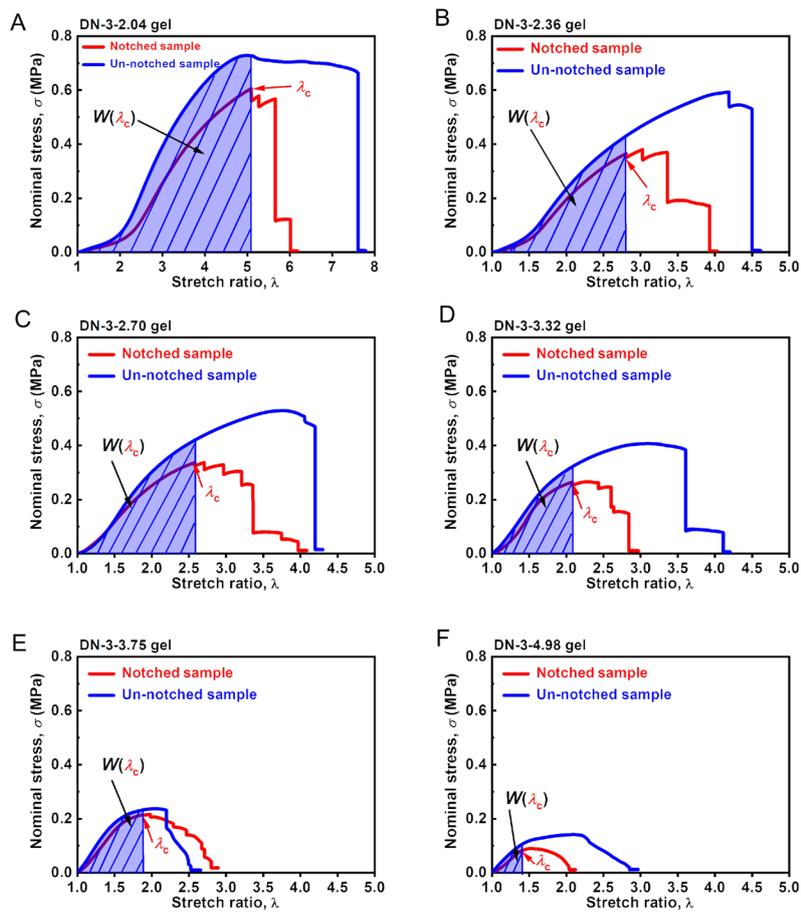
Figure S3. Typical stress curves of the notched and un-notched samples for the pure shear fracture tests. (A-F) Typical stress curves for DN-3-2.04 (A), DN-3-2.36 (B), DN-3-2.70 (C), DN-3-3.32 (D), DN-3-3.75 (E) and DN-3-4.98 (F) gels.

Calculation of elastic energy per Kuhn segment of strands $\frac{F_{el}^0}{N_x k_B T} = \frac{E\lambda_s^3}{N_x E_0} = \frac{2E\lambda_s^3}{3k_B T C_0}$

In the main text, we derived $\frac{F_{el}^0}{N_x k_B T} = \frac{E\lambda_s^3}{N_x E_0}$ (Eqn.(9)). If we assume all the first network monomers are incorporated in the elastically effective strands of the first network, we have $N_x = \frac{C_0}{v_{e,0}}$, where C_0 is the total Kuhn monomer number per volume of the elastically effective strands and $v_{e,0}$ is the number density of first network strands. In the current study, because all the first networks were prepared at the fixed monomer concentration when varying the crosslinker density, so the Kuhn monomer concentration C_0 is a constant. Because for the as-prepared SN hydrogel, we have $E_0 = \frac{3}{2}v_{e,0}k_B T$, finally we derive the equation for elastic energy per Kuhn segment of strands $\frac{F_{el}^0}{N_x k_B T} = \frac{2E\lambda_s^3}{3k_B T C_0}$. Here the Kuhn monomer concentration C_0 can be related to the monomer concentration in feed at the first network preparation C_m by this equation of $C_m = C_0 \times b/a$, where a is the characteristic length of monomer (0.25 nm, ref [S1,S2]) and b is the Kuhn length (0.5 nm, ref [S3]) for PAMPS polymer.

For Tetra-PEG gel referenced from ref [21] in the main text, elastic energy per Kuhn segment of strands was calculated based on $\frac{F_{el}^0}{N_x k_B T} = \frac{E\lambda_s^3}{N_x E_0}$. Since $\lambda_{max,0} = \frac{R_{max}}{R_0} = \frac{b\,N_x}{bN_x^{\,v}} = N_x^{\,1-v}$, assuming Gaussian strands in the as prepared reference state, $v = 0.5$ (ref [S4]), thus, $\lambda_{max,0} = N_x^{\,0.5}$. For TPEG gel, $\lambda_{max,0} = 7.6$, as noted in the reference paper (ref [S5]). So, we obtained $N_x = 57.6$.

Calculation of the theoretical stretching limit of first network strands in relative to their as prepared reference state $\lambda_{max,0}$

In the main text, we derived the equation of $\lambda_{max,0} = \frac{R_{max}}{R_0} = \frac{b\,N_x}{bN_x^{\,v}} = N_x^{\,1-v} = \left(\frac{C_0}{v_{e,0}}\right)^{1-v}$. Assuming Gaussian strands in the as prepared reference state, $v = 0.5$ (ref [S4]).

Thus, $\lambda_{max,0} = \left(\frac{C_0}{v_{e,0}}\right)^{0.5} = \left(\frac{C_m a}{bv_{e,0}}\right)^{0.5}$. Taking SN-3 gel as an example, $v_{e,0} = 3.38 \times 10^{24}$ m^{-3}, $C_m = 1 \times 1000 \times 6.02 \times 10^{23}\ m^{-3} = 6.02 \times 10^{26}$ m^{-3}, $a = 0.25$ nm, and $b = 0.5$

nm, thus, we have $\lambda_{max,0} = 9.44$. All the $\lambda_{max,0}$ for various SN gels are summarized in Table. S4.

For TPEG gel, $\lambda_{max,0} = 7.6$, as noted in the reference paper (ref [S5]).

How strain hardening characteristics affect the numerical constant γ

The crack tip stress field for the generalized neo-Hookean (GNH) soft elastic solids subjected to large deformation under Mode I plane stress conditions has been well established by the asymptotic near tip stress field analysis.[1] The true stress component τ_{22} has the following form

$$\tau_{22} = \frac{\mu}{r}\frac{b^{n-1}}{n^n}a^{2n}(1-\frac{1}{2n})^{2n}n^{1-n}(\omega(\theta,n)+\kappa\cos\theta)^{-1} \qquad (S1)$$

Here μ is the small strain shear modulus and n is the hardening coefficient. For a neo-Hookean solid, $n = 1$. Higher n means more strain hardening. Also, $\omega(\theta,n)$ and k are defined in ref [S6] as:

$$\kappa = 1 - \frac{1}{n} \qquad (S2a)$$

$$\omega(\theta,n) = \sqrt{1 - \kappa^2\sin^2\theta} \qquad (S2b)$$

The energy release rate J derived for the generalized neo-Hookean (GNH) soft elastic solids subjected to large deformation under Mode I plane stress conditions is also given by (97b) in ref [S6]. It is

$$J = \frac{\mu\pi}{2}(\frac{b}{n})^{n-1}(1-\frac{1}{2n})^{2n-1}n^{1-n}a^{2n} \qquad (S3)$$

If we substitute (S3) into (S1), we have

$$\tau_{22} = \frac{2}{n\pi}(1-\frac{1}{2n})\frac{J}{r}(\omega(\theta,n)+\kappa\cos\theta)^{-1} \qquad (S4)$$

At fracture initiation, $J = \Gamma$, (S4) becomes:

$$\tau_{22} = \underbrace{\frac{2}{n\pi}\left(1-\frac{1}{2n}\right)\left(\omega(\theta,n)+\kappa\cos\theta\right)^{-1}}_{\gamma}\frac{\Gamma}{r} \qquad (S5)$$

The bracket quantity in (S5) is our γ as defined in (10) in the main text, i.e.,

$$\gamma = \frac{2}{n\pi}(1-\frac{1}{2n})(\omega(\theta,n)+\kappa\cos\theta)^{-1} \qquad (S6)$$

Note for neo-Hookean solid where $n = 1$, $\omega(\theta,n=1) = 1$ (independent of angle) and $\kappa = 0$, so

$$\gamma = \frac{1}{\pi}$$

Hence for $n = 1$, we derived the equation of $\tau_{22} = \frac{\Gamma}{\pi r}$ in the main text.

Imagine as n increases (strain hardening), the factor $\frac{2}{n\pi}(1 - \frac{1}{2n})$ in γ in (S6) will

decrease (here we assume the term $(\omega(\theta, n) + \kappa \cos\theta)^{-1} \approx 1$, this is approximately true for a wide range of angles). For example, if $\theta = 0$, then $\omega(\theta = 0, n) = 1$ and

$\kappa \cos(\theta = 0) = 1 - \frac{1}{n}$, so $(\omega(\theta = 0, n) + \kappa)^{-1} = \left(2 - \frac{1}{n}\right)^{-1} = \frac{n}{2n-1}$.

For $\theta = \pi/2$, this factor equals $\left(\sqrt{1 - \kappa^2}\right)^{-1} = \sqrt{\frac{n}{2n-1}}$.

So in general, this term also decrease with angle.

If we take this term to be 1, then $n = 3$ will give $\gamma = \frac{2}{n\pi}(1 - \frac{1}{2n})$, so $n = 3$ gives

$$\gamma = \frac{2}{n\pi}\left(1 - \frac{1}{2n}\right)\underset{n=3}{=} \frac{5}{9\pi} \approx 0.177$$

, which is reasonably close to our observation for DN

hydrogels (~ 0.192).

SI references

(S1) Kiyama, R.; Yoshida, M.; Nonoyama, T.; Sedlačík, T.; Jinnai, H.; Kurokawa, T.; Nakajima, T.; Gong, J. P. Nanoscale TEM Imaging of Hydrogel Network Architecture. *Adv. Mater.* **2022**, 2208902.

(S2) Tanaka, Y.; Kuwabara, R.; Na, Y.-H.; Kurokawa, T.; Gong, J. P.; Osada, Y. Determination of fracture energy of high strength double network hydrogels. *The Journal of Physical Chemistry B* **2005,** 109 (23), 11559-11562.

(S3) Cui, S.; Liu, C.; Wang, Z.; Zhang, X.; Strandman, S.; Tenhu, H. Single molecule force spectroscopy on polyelectrolytes: effect of spacer on adhesion force and linear charge density on rigidity. *Macromolecules* **2004,** 37 (3), 946−953.

(S4) Rubinstein, M.; Colby, R. H., *Polymer physics*. Oxford university press New York: 2003; Vol. 23;

(S5) Matsuda, T.; Nakajima, T.; Fukuda, Y.; Hong, W.; Sakai, T.; Kurokawa, T.; Chung, U.-i.; Gong, J. P. Yielding criteria of double network hydrogels. *Macromolecules* **2016,** 49, 1865−1872.

(S6) Long, R.; Hui, C.-Y. Crack tip fields in soft elastic solids subjected to large quasi-static deformation—a review. *Extreme Mechanics Letters* **2015**, 4, 131−155.